A Nonlinear Constituent Based Viscoelastic Model for Articular Cartilage and Analysis of Tissue Remodeling Due to Altered Glycosaminoglycan-Collagen Interactions

Gregory C. Thomas
Department of Mechanical Engineering,
California Polytechnic State University,
San Luis Obispo, CA 93407

Anna Asanbaeva
Department of Bioengineering,
University of California-San Diego,
La Jolla, CA 92093

Pasquale Vena
Department of Structural Engineering,
Laboratory of Biological Structure Mechanics,
Politecnico di Milano,
20133, Milan, Italy

Robert L. Sah
Department of Bioengineering,
University of California-San Diego,
La Jolla, CA 92093

Stephen M. Klisch[1]
Associate Professor
Department of Mechanical Engineering,
California Polytechnic State University,
San Luis Obispo, CA 93407
e-mail: sklisch@calpoly.edu

*A constituent based nonlinear viscoelastic (VE) model was modified from a previous study (Vena, et al., 2006, "A Constituent-Based Model for the Nonlinear Viscoelastic Behavior of Ligaments," J. Biomech. Eng., **128**, pp. 449–457) to incorporate a glycosaminoglycan (GAG)-collagen (COL) stress balance using compressible elastic stress constitutive equations specific to articular cartilage (AC). For uniaxial loading of a mixture of quasilinear VE constituents, time constant and relaxation ratio equations are derived to highlight how a mixture of constituents with distinct quasilinear VE properties is one mechanism that produces a nonlinear VE tissue. Uniaxial tension experiments were performed with newborn bovine AC specimens before and after ~55% and ~85% GAG depletion treatment with guanidine. Experimental tissue VE parameters were calculated directly from stress relaxation data, while intrinsic COL VE parameters were calculated by curve fitting the data with the nonlinear VE model with intrinsic GAG viscoelasticity neglected. Select tissue and intrinsic COL VE parameters were significantly different from control and experimental groups and correlated with GAG content, suggesting that GAG-COL interactions exist to modulate tissue and COL mechanical properties. Comparison of the results from this and other studies that subjected more mature AC tissue to GAG depletion treatment suggests that the GAGs interact with the COL network in a manner that may be beneficial for rapid volumetric expansion during developmental growth while protecting cells from excessive matrix strains. Furthermore, the underlying GAG-COL interactions appear to diminish as the tissue matures, indicating a distinctive remodeling response during developmental growth.*
[DOI: 10.1115/1.3192139]

Keywords: cartilage, collagen, viscoelastic, glycosaminoglycans, remodeling

1 Introduction

Articular cartilage (AC) covers the ends of articulating bones in synovial joints and functions to transmit loads during joint motion with minimal friction. Approximately 60–80% of AC wet weight (WW) is interstitial fluid [1] and the remaining weight is a porous solid matrix (SM) composed of glycosaminoglycans (GAGs), collagens (COLs), and other noncollagenous proteins [2]. GAGs provide a fixed negative charge that causes the SM to swell and resist compressive loads and a predominantly type II COL crosslinked network resists tensile and shear loads [3].

The long-term goals of this study include improving structure-function relations among biochemical, molecular, and mechanical properties that may be used in continuum mechanics models of AC growth and remodeling [4,5]. A major obstacle is that AC mechanical properties are difficult to model at the continuum level due to their complexity; they vary in location [2] and depth from the articular surface [6], exhibit anisotropy with respect to directions relative to anatomical split-line direction [7], and exhibit strong tension-compression asymmetry [8,9]. AC tissue is likely to experience finite, multidimensional strains when subject to typical loads in vivo [10,11]. These observations suggest the need for finite deformation (i.e., nonlinear) anisotropic stress constitutive equations.

Furthermore, an AC generally exhibits both fluid flow-dependent and flow-independent (i.e., intrinsic) viscoelastic (VE) behavior [12–17]. With regard to uniaxial tension (UT) stress relaxation, all VE models have a relaxation response that can be described by a time constant τ and a relaxation ratio R. Linear and nonlinear VE models may be characterized by τ and R parameters that are strain independent and strain dependent, respectively, while in the quasilinear VE model [18] R, but not τ, is strain dependent [19].[2] AC tissue VE models employed linear [16,20,21], quasilinear [12,14], and nonlinear [17,22] viscoelasticity yet none of these formulations used anisotropic elastic stress equations for finite deformations. Recently, Vena et al. [23] introduced a constituent based VE model employing a mixture of quasilinear VE constituents with anisotropic elastic stress equations for finite deformations. That study showed that a mixture of quasilinear VE constituents leads to a nonlinear tissue VE response

[1]Corresponding author.

Contributed by the Bioengineering Division of ASME for publication in the JOURNAL OF BIOMECHANICAL ENGINEERING. Manuscript received November 15, 2008; final manuscript received June 3, 2009; published online September 1, 2009. Review conducted by Michael Sacks.

[2]These differences are discussed in more detail in Secs. 2 and 4.

suggesting one mechanism that causes nonlinear VE behavior. The first objective of this study was to modify the model in Ref. [23] to incorporate, and thereby allow study of, AC viscoelasticity.

Previous studies suggested that VE parameters may change following GAG depletion for AC [24–29] and other biological tissues such as lung tissue [30], temporomandibular joint disk tissue [31], tendon tissue [32], and mitral valve tissue [33]. While most GAG depletion studies with AC involved the use of mature tissue, a recent study [29] suggested that GAG-COL interactions regulate tissue VE properties in a manner dependent on the tissue's maturational stage. In order to illustrate how a constituent based VE model may be used to improve delineation of AC structure-function relations in tissue growth and remodeling, the second objective of this study was to quantify the VE response for control and GAG depleted immature (i.e., newborn) bovine AC tested in UT. Including the comparison of the results with other studies with more mature AC tissue, this objective serves as a first step toward developing a better understanding of how AC remodels during developmental growth to modulate tissue VE properties.

In UT, the effects of flow-dependent viscoelasticity and intrinsic GAG viscoelasticity may be neglected as suggested in several previous studies [22,34–37][3]. Consequently, the use of such a simplified model with UT experiments facilitates the investigation of several GAG-COL interactions on both tissue and COL VE properties. Here, *indirect* GAG interactions are defined as those that result from a reduction in GAG swelling pressure and a resultant elastic relaxation of the prestressed COL network arising from a GAG-COL stress balance, and *direct* GAG interactions are defined as those that arise due to both covalent and noncovalent molecular interactions between GAGs and the COL network.

The specific aims are (1) to develop a constituent based nonlinear VE model specific to AC, (2) to perform UT stress relaxation experiments for both fresh and GAG depleted immature AC specimens, and (3) to quantify both experimental tissue and intrinsic COL VE parameters and assess whether significant changes occur due to GAG depletion and if correlations with GAG and COL contents exist.

2 Methods

2.1 Theory

2.1.1 Preliminaries. In this work, the AC SM is assumed to occupy a reference configuration κ_0 at time t_0 and a configuration κ at time t, such that κ_0 and κ represent equilibrium and nonequilibrium states, respectively. The right Cauchy–Green deformation tensor $\mathbf{C}$ is

$$\mathbf{C} = \mathbf{F}^T\mathbf{F} \tag{1}$$

where $\mathbf{F}$ is the deformation gradient tensor and T the transpose operator. The elastic second Piola–Kirchhoff stress $\mathbf{S}$ is derived from a strain energy function W as

$$\mathbf{S} = 2\frac{\partial W}{\partial \mathbf{C}} \tag{2}$$

and is related to Cauchy stress $\mathbf{T}$ or first Piola–Kirchhoff stress $\mathbf{P}$ using

$$J\mathbf{T} = \mathbf{F}\mathbf{S}\mathbf{F}^T = \mathbf{P}\mathbf{F}^T \tag{3}$$

where the Jacobian J is the determinant of $\mathbf{F}$, i.e., $J=\det(\mathbf{F})$.

2.1.2 Stress Balance Hypothesis and Elastic Constitutive Laws. A GAG-COL stress balance is assumed such that SM stress $\mathbf{S}$ is the sum of the GAG ($\mathbf{S}^{\mathrm{GAG}}$) and COL ($\mathbf{S}^{\mathrm{COL}}$) stresses at every time t,[4]

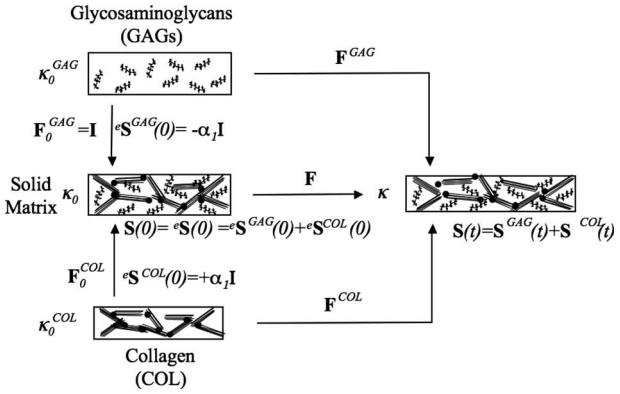

Fig. 1 The stress balance hypothesis. The GAG and COL constituents have their own reference configurations, κ_0^{GAG} and κ_0^{COL}. The GAG constituent has the same configuration in κ_0^P and κ_0, which is equivalent to $\mathbf{F}_0^{GAG}=\mathbf{I}$ and ${}^e\mathbf{S}^{GAG}(0)=-\alpha_1\mathbf{I}$. To balance this swelling stress, the COL network supports a tensile prestress produced by an initial COL deformation gradient tensor $\mathbf{F}_0^{COL}$, which yields the initial collagen stress tensor ${}^e\mathbf{S}^{COL}(0)=\alpha_1\mathbf{I}$. After a deformation F is applied, the constituent stresses are calculated relative to their respective reference configurations and using $\mathbf{F}^{GAG}=\mathbf{F}\mathbf{F}_0^{GAG}$ and $\mathbf{F}^{COL}=\mathbf{F}\mathbf{F}_0^{COL}$.

$$\mathbf{S}(t) = \mathbf{S}^{\mathrm{GAG}}(t) + \mathbf{S}^{\mathrm{COL}}(t) \tag{4}$$

Full details of the elastic stress equations are presented in Appendix A. Briefly, the elastic GAG stress ${}^e\mathbf{S}^{\mathrm{GAG}}$ is based on a two compartmental (i.e., extra- and intrafibrillar water compartments) isotropic swelling stress model originally proposed in Ref. [38] and used in Refs. [5,39] to derive a continuum level GAG stress equation with material constants α_1 and α_2. The elastic COL stress ${}^e\mathbf{S}^{\mathrm{COL}}$ is based on Ref. [40] and contains both an isotropic component ${}^e\mathbf{S}^0$ with material constant μ and an anisotropic bimodular fiber-reinforced component ${}^e\mathbf{S}^{\mathrm{BIM}}$ with material constants γ_1, γ_2, γ_3, and δ, which are active (i.e., nonzero) only when their corresponding fibers are in tension.

The GAG and COL constituents are allowed to have distinct reference configurations, κ_0^{GAG} and κ_0^{COL} (Fig. 1). Each constituent is then prescribed an initial deformation, $\mathbf{F}_0^{\mathrm{GAG}}$ and $\mathbf{F}_0^{\mathrm{COL}}$, to map it to the SM reference configuration κ_0. The SM occupies a stress-free equilibrium reference configuration at time $t=0$, i.e., $\mathbf{S}(0)={}^e\mathbf{S}(0)=\mathbf{0}$. However, the GAG isotropic swelling stress model does not have a stress-free configuration. Here, the GAG constituent has the same configuration in κ_0^{GAG} and κ_0, which is equivalent to $\mathbf{F}_0^{\mathrm{GAG}}=\mathbf{I}$ and from Eq. (A1) ${}^e\mathbf{S}^{\mathrm{GAG}}(0)=-\alpha_1\mathbf{I}$.[5] To balance this swelling stress, the COL network must support a tensile prestress produced by an initial COL deformation gradient tensor $\mathbf{F}_0^{\mathrm{COL}}$, which yields the initial collagen stress tensor, ${}^e\mathbf{S}^{\mathrm{COL}}(0)=\alpha_1\mathbf{I}$. $\mathbf{F}_0^{\mathrm{COL}}$ can be determined from Eqs. (A3) and (A7). After a deformation $\mathbf{F}$ is applied, the constituent stresses are calculated relative to their respective reference configurations using

$$\mathbf{F}^{\mathrm{GAG}} = \mathbf{F}\mathbf{F}_0^{\mathrm{GAG}}, \quad \mathbf{F}^{\mathrm{COL}} = \mathbf{F}\mathbf{F}_0^{\mathrm{COL}} \tag{5}$$

2.1.3 Constituent Based Viscoelasticity. To implement constituent based viscoelasticity, the method of Ref. [23] for each constituent stress in Eq. (4) is implemented as[6]

[3]These assumptions are discussed further in Sec. 4.

[4]In Eq. (4), stresses are VE stresses; a superscript e will be used to designate elastic stresses.

[5]Equation numbers preceded by "A" and "B" refer to those in Appendices A and B.

[6]VE models usually include a term for strain rate (i.e., $d\mathbf{E}/dt$) inside the convolution integral to account for the dependence on strain rate. As stress is proportional to strain, the dependence on strain rate can also be achieved with a stress rate term $d\mathbf{S}/dt$ [23].

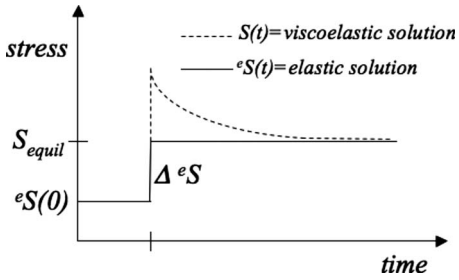

Fig. 2 Stress response to a step increase in strain and, consequently, a step increase in elastic stress $\Delta^e S$ at time $t_{step}>0$ with initial equilibrium elastic stress $^eS(0)$

$$\mathbf{S}(t) = {}^e\mathbf{S}^{\mathrm{GAG}}(0) + \int_0^t G^{\mathrm{GAG}}(t-\tau)\frac{d\,{}^e\mathbf{S}^{\mathrm{GAG}}}{d\tau}d\tau + {}^e\mathbf{S}^{\mathrm{COL}}(0) + \int_0^t G^{\mathrm{COL}}(t-\tau)\frac{d\,{}^e\mathbf{S}^{\mathrm{COL}}}{d\tau}d\tau \tag{6}$$

Two different relaxation functions, G^{GAG} and G^{COL}, allow each constituent to have its own VE behavior. The relaxation functions are evaluated as a Prony series of exponential terms [20,23]

$$G^{\mathrm{GAG}}(t) = 1 + \sum_{i=1}^{n} g_i^{\mathrm{GAG}} \exp(-t/\tau_i^{\mathrm{GAG}})$$
$$G^{\mathrm{COL}}(t) = 1 + \sum_{i=1}^{n} g_i^{\mathrm{COL}} \exp(-t/\tau_i^{\mathrm{COL}}) \tag{7}$$

where τ_i and g_i are called constituent time constants and amplification coefficients, respectively.

2.1.4 Stress Response to a Step Increase in Strain. In this study, τ_i and g_i are assumed strain independent to represent quasilinear constituent viscoelasticity. However, the constituent based VE model renders nonlinear tissue viscoelasticity with strain-dependent tissue time constant and relaxation ratios, as derived below for a step increase in strain. To simplify the derivation, only the stress S for uniaxial loading with a single constituent will be considered, thus Eq. (6) reduces to

$$S(t) = {}^eS(0) + \int_0^t G(t-\tau)\frac{d^eS}{d\tau}d\tau \tag{8}$$

Consider the stress response to a step increase in strain and, consequently, a step increase in elastic stress $\Delta^e S$ at time $t_{step}>0$ with initial equilibrium elastic stress $^eS(0)$ (Fig. 2). For this special case, the following equation for the stress at $t \geq t_{step}$ is obtained in Appendix B:[7]

$$S(t) = {}^eS(0) + \Delta^eS + \Delta^eS\sum_{i=1}^{n} g_i \exp\left(\frac{-(t-t_{step})}{\tau_i}\right) \tag{9}$$

2.1.5 Relation Between Tissue and Constituent Time Constants. The tissue time constant τ is defined as the amount of time t it takes for the tissue stress to relax by 63.2% from its peak value $S(t_{step})$ following a step increase in strain and can be calculated from

$$S(\tau) = S_{equil} + 0.368(S(t_{step}) - S_{equil}) \tag{10}$$

where the equilibrium stress is

$$S_{equil} = {}^eS^{\mathrm{GAG}}(0) + \Delta\,{}^eS^{\mathrm{GAG}} + {}^eS^{\mathrm{COL}}(0) + \Delta\,{}^eS^{\mathrm{COL}} \tag{11}$$

The peak stress is obtained upon evaluating Eq. (9) at $t=t_{step}$ for each constituent

$$S(t_{step}) = {}^eS^{\mathrm{GAG}}(0) + \Delta\,{}^eS^{\mathrm{GAG}}\left(1 + \sum_{i=1}^{n} g_i^{\mathrm{GAG}}\right) + {}^eS^{\mathrm{COL}}(0) + \Delta\,{}^eS^{\mathrm{COL}}\left(1 + \sum_{i=1}^{n} g_i^{\mathrm{COL}}\right) \tag{12}$$

Using Eqs. (11) and (12) in Eq. (10) yields

$$S(\tau) = S_{equil} + 0.368\left(\Delta\,{}^eS^{\mathrm{GAG}}\sum_{i=1}^{n} g_i^{\mathrm{GAG}} + \Delta\,{}^eS^{\mathrm{COL}}\sum_{i=1}^{n} g_i^{\mathrm{COL}}\right) \tag{13}$$

Evaluating Eq. (9) at $t=\tau$ for each constituent and using Eq. (11) one obtains

$$S(\tau) = S_{equil} + \Delta\,{}^eS^{\mathrm{GAG}}\sum_{i=1}^{n} g_i^{\mathrm{GAG}} \exp\left(\frac{-(\tau-t_{step})}{\tau_i^{\mathrm{GAG}}}\right) + \Delta\,{}^eS^{\mathrm{COL}}\sum_{i=1}^{n} g_i^{\mathrm{COL}} \exp\left(\frac{-(\tau-t_{step})}{\tau_i^{\mathrm{COL}}}\right) \tag{14}$$

Equating Eqs. (13) and (14) allows the calculation of τ from

$$0.368\left(\Delta\,{}^eS^{\mathrm{GAG}}\sum_{i=1}^{n} g_i^{\mathrm{GAG}} + \Delta\,{}^eS^{\mathrm{COL}}\sum_{i=1}^{n} g_i^{\mathrm{COL}}\right) = \Delta\,{}^eS^{\mathrm{GAG}}\sum_{i=1}^{n} g_i^{\mathrm{GAG}} \exp\left(\frac{-(\tau-t_{step})}{\tau_i^{\mathrm{GAG}}}\right) + \Delta\,{}^eS^{\mathrm{COL}}\sum_{i=1}^{n} g_i^{\mathrm{COL}} \exp\left(\frac{-(\tau-t_{step})}{\tau_i^{\mathrm{COL}}}\right) \tag{15}$$

For a single constituent Eq. (15) reduces to

$$0.368\sum_{i=1}^{n} g_i = \sum_{i=1}^{n} g_i \exp\left(\frac{-(\tau-t_{step})}{\tau_i}\right) \tag{16}$$

which reveals that when the relaxation function parameters are constants, τ is strain independent, a characteristic of quasilinear viscoelasticity. Conversely, for constituent based viscoelasticity Eq. (15) reveals that τ depends on the applied UT strain (because of the dependence on stress in Eq. (15)) a characteristic of nonlinear viscoelasticity.

2.1.6 Relation Between Tissue and Constituent Relaxation Ratios. The relaxation ratio R is defined as equilibrium stress divided by peak stress

$$R = \frac{S_{equil}}{S(t_{step})} \tag{17}$$

Using Eqs. (11) and (12) in Eq. (17) yields

[7]Note that as $t\to\infty$, $S(t)$ is the equilibrium (elastic) stress $^eS(0)+\Delta^eS$.

$$R = \frac{{}^{e}S^{\mathrm{GAG}}(0) + \Delta\ {}^{e}S^{\mathrm{GAG}} + {}^{e}S^{\mathrm{COL}}(0) + \Delta\ {}^{e}S^{\mathrm{COL}}}{{}^{e}S^{\mathrm{GAG}}(0) + \Delta {}^{e}S^{\mathrm{GAG}}\left(1 + \sum_{i=1}^{n} g_i^{\mathrm{GAG}}\right) + {}^{e}S^{\mathrm{COL}}(0) + \Delta\ {}^{e}S^{\mathrm{COL}}\left(1 + \sum_{i=1}^{n} g_i^{\mathrm{COL}}\right)} \tag{18}$$

For a single constituent Eq. (18) reduces to

$$R = \frac{{}^{e}S(0) + \Delta {}^{e}S}{{}^{e}S(0) + \Delta {}^{e}S\left(1 + \sum_{i=1}^{n} g_i\right)} \tag{19}$$

which reveals that when the relaxation function parameters are constants, R is strain dependent as it is a function of applied UT strain when the initial strain is not zero, a characteristic of quasilinear viscoelasticity.[8] For constituent based viscoelasticity, Eq. (18) reveals how R additionally depends on the constituent properties.

2.1.7 Time Discretization Procedure. In the current study, the method of Ref. [23] is modified in three ways. (1) The initial equilibrium elastic stresses of the constituents, ${}^{e}\mathbf{S}^{\mathrm{GAG}}(0)$ and ${}^{e}\mathbf{S}^{\mathrm{COL}}(0)$, are nonzero in a SM stress-free reference configuration; (2) the first term in the relaxation functions equals 1 instead of a variable g_∞ so that the equilibrium elastic stress is obtained as $t \to \infty$; and (3) the incompressibility assumption is not used. These modifications result in a slightly different time discretization scheme summarized here.[9]

To simplify the final result, a recursive expression for time-dependent matrices $\mathbf{c}^i(t)$ and a scalar c^{COL} specific to COL are defined as

$$\mathbf{c}^i(t) = \exp(-\Delta t/\tau_i^{\mathrm{COL}})\mathbf{c}^i(t - \Delta t) + g_i^{\mathrm{COL}}\tau_i^{\mathrm{COL}}(1 - \exp(-\Delta t/\tau_i^{\mathrm{COL}}))\left(\frac{{}^{e}\mathbf{S}^{\mathrm{COL}}(t) - {}^{e}\mathbf{S}^{\mathrm{COL}}(t - \Delta t)}{\Delta t}\right) \tag{20}$$

and

$$c^{\mathrm{COL}} = 1 + \frac{1}{\Delta t}\sum_{i=1}^{n} g_i^{\mathrm{COL}}\tau_i^{\mathrm{COL}}(1 - \exp(-\Delta t/\tau_i^{\mathrm{COL}})) \tag{21}$$

The time discretization procedure used to calculate $\mathbf{S}^{\mathrm{COL}}(t+\Delta t)$ after a time increment Δt is

$$\mathbf{S}^{\mathrm{COL}}(t + \Delta t) = (c^{\mathrm{COL}}){}^{e}\mathbf{S}^{\mathrm{COL}}(t + \Delta t) + (1 - c^{\mathrm{COL}}){}^{e}\mathbf{S}^{\mathrm{COL}}(t) + \sum_{i=1}^{n} \exp(-\Delta t/\tau_i^{\mathrm{COL}})\mathbf{c}^i(t) \tag{22}$$

An analogous expression may be obtained for the GAG constituent.

2.1.8 A Model for UT and Aggregate COL VE Parameters. For UT analysis, GAG viscoelasticity is neglected upon assuming that the AC UT VE response is dominated by intrinsic COL viscoelasticity.[10] The *UT model* is obtained by setting all GAG relaxation parameters g_i^{GAG} equal to zero. As seen below, a different number of Prony series terms for the COL relaxation function are needed for different experimental groups, thus, it is not possible to investigate significant differences for g_i^{COL} and τ_i^{COL} between groups. Instead, an aggregate COL time constant and an aggregate COL relaxation ratio are defined as functions of g_i^{COL} and τ_i^{COL} to render COL viscous properties that may be compared between groups with different number of relaxation function terms.

For the UT model, the amount of time $t = \tau_A^{\mathrm{COL}}$ it takes to relax by 63.2% can be calculated from Eq. (15), which reduces upon neglecting intrinsic GAG VE to

$$0.368\sum_{i=1}^{n} g_i^{\mathrm{COL}} = \sum_{i=1}^{n} g_i^{\mathrm{COL}} \exp\left(\frac{-(\tau_A^{\mathrm{COL}} - t_{\mathrm{step}})}{\tau_i^{\mathrm{COL}}}\right) \tag{23}$$

where τ_A^{COL} is defined as the *aggregate COL time constant*. The relaxation ratio R from Eq. (16) reduces upon neglecting intrinsic GAG VE and using a SM stress free reference configuration to

$$R = \frac{\Delta\ {}^{e}S^{\mathrm{GAG}} + \Delta\ {}^{e}S^{\mathrm{COL}}}{\Delta\ {}^{e}S^{\mathrm{GAG}} + \Delta\ {}^{e}S^{\mathrm{COL}}\left(1 + \sum_{i=1}^{n} g_i^{\mathrm{COL}}\right)} \tag{24}$$

suggesting a definition for an *aggregate* COL relaxation ratio R_A^{COL} as[11]

$$R_A^{\mathrm{COL}} = \frac{1}{1 + \sum_{i=1}^{n} g_i^{\mathrm{COL}}} \tag{25}$$

Recall that, relative to a stress- and strain-free configuration, the time constant and relaxation ratio depend on the applied UT strain for a nonlinear VE material but do not depend on the applied UT strain for a quasilinear VE material. Thus, for the UT model, Eqs. (24) and (23) reveal that the relaxation ratio, but not the time constant, depends on the applied UT strain. Consequently, this model falls somewhere between nonlinear and quasilinear viscoelasticity.

2.2 Experiments. From an earlier study [41], the UT stress relaxation response was measured on groups of adjacent paired AC explants having 0%, ~55%, and ~85% GAG depletion. Newborn (1–3 week old) bovine AC patellofemoral groove explants were harvested from ~0.6 mm below the AC surface and sliced to a thickness of ~0.25 mm. Twelve explants were harvested corresponding to four specimens per group. The control group (no GAG depletion, i.e., GD-0) did not receive enzyme treatment. The explants for the ~85% GAG extraction group (GD-85) were rinsed in guanidine HCl (Gnd) to remove ~85% GAG mass. The explants for the ~55% GAG extraction group (GD-55) were rinsed in Gnd to remove ~85% GAG mass and then soaked in a solution of Gnd saturated with cartilage extract to replete GAG mass to ~45% of the average GD-0 GAG mass.

Explants were punched into tapered tensile specimens (length ~4 mm and cross-sectional gauge area of $\sim 0.25 \times 0.8$ mm^2) and oriented such that the direction of uniaxial loading was along the anterior-posterior direction, approximately perpendicular to the split-line direction [42]. The thickness of each tensile specimen was measured at three locations in the gauge region and averaged

[8] Note that relative to a zero stress-zero strain configuration, R defined by Eq. (19) is strain independent, which is also a characteristic of quasilinear viscoelasticity.

[9] The derivation is nearly identical to that in Ref. [23] and the reader is referred to that paper for full details.

[10] This assumption is discussed further in Sec. 4.

[11] Equation (25) defines a viscous material constant that is independent of strain, decoupling elastic and viscous properties and is preferable to Eq. (24), which couples elastic and viscous properties, for statistical analysis of COL viscous properties.

for cross-sectional area calculations. The specimens were loaded into a testing fixture, pulled to a tare-load of 0.05 N (equivalent to a stress of ~0.2 MPa), allowed to relax, and then pulled to 10% strain under displacement control over a 40 s ramp. Displacement was held at 10% strain during a 900 s stress relaxation period. The measured load and displacement were converted to first Piola–Kirchhoff stress (load/original cross-sectional area) and strain (elongation/initial clamp to clamp distance).

Each tensile specimen and residual tissue obtained during preparation were saved for biochemical analysis. Samples were solubilized with proteinase K [43] and analyzed to quantify content of sulfated GAG [44] and hydroxyproline [45]. Hydroxyproline content was converted to COL content by assuming a mass ratio of COL/hydroxyproline=7.25 for bovine cartilage [46,47]. Biochemical parameters were normalized to tissue wet weight to represent constituent content.

2.3 Parameter Estimation

2.3.1 Experimental Tissue VE Parameters. Experimental stress data were used to calculate experimental tissue VE parameters that are independent of the proposed VE model. Equilibrium stress was defined as the stress at the end of the relaxation phase. Experimental Young's modulus $E^{\exp}$ was defined as equilibrium stress divided by applied strain (0.10). The experimental time constant $\tau^{\exp}$ was defined as the amount of time it takes for the stress to relax by 63.2% from the peak stress that occurs at the end of the ramp phase. The experimental relaxation ratio $R^{\exp}$ was defined as equilibrium stress/peak stress.

2.3.2 Elastic Material Properties. Experimental stress and biochemical data were used to calculate elastic GAG-COL parameters in elastic constitutive equations using MATLAB. GAG material constants α_1 and α_2 Eq. (A1) were calculated using an extended two compartment (i.e., extra- and intrafibrillar water) swelling stress model for AC GAGs developed by Basser et al. [38] and extended by Klisch and co-workers [5,39]. For each specimen, biochemical mass measurements were used to calculate GAG swelling stress (normalized to extrafibrillar water area), which is then converted to GAG Cauchy stress (normalized to tissue area). It was assumed that one set of parameters is a valid description for the GAG stress-density relations for each group, therefore, the four specimens for each group were pooled together to curve fit the theoretical GAG Cauchy stress, $\mathbf{T}^{\mathrm{GAG}}=-\alpha_1^*(\rho^{\mathrm{GAG}})^{\alpha_2}\mathbf{I}$ to yield parameters α_1^* and α_2. The parameter α_1 was calculated using $\alpha_1=\alpha_1^*(\rho_0^{\mathrm{GAG}})^{\alpha_2}$ and the continuity equation $\rho^{\mathrm{GAG}}J^{\mathrm{GAG}}=\rho_0^{\mathrm{GAG}}$ and Eq. (3) was used to obtain ${}^e\mathbf{S}^{\mathrm{GAG}}$ (Eq. (A1)).

Due to a lack of comprehensive data, the COL elastic parameters (μ, Φ_{+12}, Φ_{+13}, and Φ_{+23}) were held constant among all specimens. In this model, μ corresponds to the tissue shear modulus for small strain elasticity theory and was estimated from torsional shear data for newborn bovine AC [48] as 0.11 MPa. The values of Φ_{+12}, Φ_{+13}, and Φ_{+23} were obtained from Refs. [5,40] as 45 deg, 35 deg, and 35 deg, respectively, which produce reasonable predictions for anisotropic and asymmetric Young's moduli and Poisson's ratios for newborn bovine and adult human AC. The remaining elastic COL material constants were constrained by $\gamma_1=\gamma_2=2\gamma_3=\delta$, which produce reasonable predictions for mechanical properties of newborn bovine AC [5]. Consequently, there remains only one adjustable COL elastic parameter, γ_1, which was calculated on a specimen-specific basis. Specifically, a MATLAB code was developed that solves for the initial COL deformation gradient tensor $\mathbf{F}_0^{\mathrm{COL}}$ and γ_1 that yields a SM stress-free reference configuration (i.e., $\mathbf{S}(0)=\mathbf{0}$), and matches the measured equilibrium stress at 10% strain.

2.3.3 Viscous Material Properties. After determining $\mathbf{F}_0^{\mathrm{COL}}$ and γ_1, the VE time discretization procedure (Eqs. (20)–(22)) with two terms in the Prony series for the COL relaxation function were coded in MATLAB to solve the UT boundary-value problem with traction free boundary conditions on the free surfaces using first Piola–Kirchhoff stress. For each specimen, an iterative optimization procedure was implemented to determine COL VE parameters (τ_1^{COL}, g_1^{COL}, τ_2^{COL}, and g_2^{COL}) that minimize the squared sum of residual errors between experimental and theoretical stress values. A parameter study revealed that the optimal solution for the GD-0 and GD-55 groups did not depend on initial guesses for (τ_1^{COL}, g_1^{COL}, τ_2^{COL}, and g_2^{COL}). However, the solution did depend on initial guesses for the GD-85 group. Consequently, for GD-85 specimens one term in the Prony series for the COL relaxation function was used.[12] After optimization, the aggregate time constant τ_A^{COL} and relaxation ratio R_A^{COL} were calculated using Eqs. (23) and (25), respectively.

2.4 Parameter Studies. A parameter study was conducted in order to differentiate between effects of the different GAG-COL interaction mechanisms on the tissue VE response. The MATLAB code was modified to obtain the UT boundary-value problem solution using first Piola–Kirchhoff stress and averaged values of the elastic and viscous parameters for the GD-0 group to identify a baseline case. Additional solutions were obtained to model progressive changes to the GD-0 VE properties due to treatment. First, the effect of an altered GAG-COL stress balance due to reduced GAG content on tissue VE properties were isolated: Averaged GAG elastic parameters (α_1, α_2) were adjusted to the GD-55 and GD-85 values while the COL VE parameters were kept equal to the GD-0 values. Second, the incremental effect of direct GAG interactions on COL elasticity was isolated: In addition to α_1 and α_2, averaged COL elastic parameters (γ_1) were adjusted to the GD-55 and GD-85 values while the COL viscous parameters were kept equal to the GD-0 values. Third, the incremental effect of direct GAG interactions on COL viscous properties was isolated: In addition to α_1, α_2, and γ_1, the COL viscous parameters τ_1^{COL}, g_1^{COL}, τ_2^{COL}, and g_2^{COL} were adjusted resulting in simulations using averaged values for all elastic and viscous parameters for the GD-55 and GD-85 groups.

2.5 Statistical Analysis. The effects of GAG depletion treatment on experimental tissue VE parameters ($E^{\exp}$, $\tau^{\exp}$, and $R^{\exp}$), aggregate VE parameters (τ_A^{COL}, R_A^{COL}), and COL elastic parameter (γ_1) were assessed using analysis of variance (ANOVA) with posthoc Tukey testing. Since a lesser number of COL viscous parameters were needed to obtain unique solutions for the GD-85 group, they were not directly compared with the GD-0 and GD-55 group values. Consequently, the effects of GAG depletion on COL viscous parameters τ_1^{COL}, g_1^{COL}, τ_2^{COL}, and g_2^{COL} were compared using paired *t*-tests for the GD-0 and GD-55 groups only. Correlations between all VE parameters with GAG and COL contents were investigated using linear regression with a *t*-test analysis of the regression slope. For all statistical analyses, a 0.05 probability of type-1 error was assumed ($p=0.05$).

3 Results

Experimental tissue VE parameters ($E^{\exp}$, $\tau^{\exp}$, and $R^{\exp}$) increased ($p<0.01$), decreased ($p<0.001$), and increased ($p<0.001$), respectively, due to increasing GAG depletion treatment (Table 1; Fig. 3). All three ($E^{\exp}$, $\tau^{\exp}$, and $R^{\exp}$) were significantly correlated with GAG content ($p<0.05$, 0.01, and 0.0001, respectively) but not COL content, although positive trends with COL existed for $E^{\exp}$ ($R^2=0.17$, $p=0.19$) and $R^{\exp}$ ($R^2=0.21$, $p=0.13$) (Fig. 4).

Unique VE model parameters for the GD-0 and GD-55 specimens were obtained with two Prony series terms in the COL relaxation function; as mentioned above, unique solutions for the

[12]For GD-85 specimens, the COL VE parameters (τ_1^{COL}, g_1^{COL}) were independent of initial guesses.

Table 1 Experimental GAG and COL contents normalized to tissue WW, GAG elastic material parameters (α_1, α_2), COL VE parameters (γ_1, τ_1^{COL}, g_1^{COL}, τ_2^{COL}, and g_2^{COL}), and curve fit R^2 values; mean+1 standard deviation values were shown; GD-0 is the control group with no GAG depletion; GD-55 and GD-85 are experimental groups with ~55% and 85% GAG depletion, respectively.

	Group		
Parameter	GD-0	GD-55	GD-85
GAG/WW (mg/g)	33.6 ± 5.6	14.6 ± 1.6	7.4 ± 1.4
COL/WW (mg/g)	87.8 ± 5.6	85.9 ± 15.7	106.6 ± 15.8
α_1 (MPa)	0.213	0.044	0.015
α_2	2.53	1.56	2.69
γ_1 (MPa)	2.91 ± 1.3	4.77 ± 1.1	11.0 ± 3.1
τ_1^{COL} (s)	30.7 ± 11.1	23.6 ± 1.1	82.2 ± 25.6
g_1^{COL}	1.10 ± 0.76	0.81 ± 0.08	0.28 ± 0.05
τ_2^{COL} (s)	312.1 ± 54.3	383.2 ± 53.2	N/A
g_2^{COL}	0.80 ± 0.15	0.28 ± 0.03	N/A
R^2	0.97 ± 0.04	0.99 ± 0.00	0.99 ± 0.00

GD-85 specimens were obtained with one Prony series term (Table 1, Fig. 5). The COL elastic parameter γ_1 increased due to increasing GAG depletion treatment ($p<0.001$) (Table 1; Fig. 6). The COL VE parameter g_2^{COL} decreased due to increasing GAG depletion treatment ($p<0.01$) (Table 1; Fig. 6), while a significant difference was almost detected for τ_2^{COL} ($p=0.06$) (Table 1; Fig. 6). The aggregate VE relaxation parameter R_A^{COL} increased due to increasing GAG depletion treatment ($p<0.0001$) while a significant difference was almost detected for τ_A^{COL} ($p=0.08$) (Fig. 6). The VE parameters (γ_1, g_2^{COL}, and R_A^{COL}) were significantly correlated with GAG content ($p<0.01$, 0.0001, and 0.001, respectively) (Fig. 7). None of the VE parameters were significantly correlated with COL content although positive trends existed for γ_1 ($R^2=0.19$, $p=0.15$) and R_A^{COL} ($R^2=0.25$, $p=0.10$) (Fig. 7).

The parameter studies using averaged GAG elastic parameters (α_1, α_2) for the GD-55 and GD-85 groups with COL VE parameters (γ_1, τ_1^{COL}, g_1^{COL}, τ_2^{COL}, and g_2^{COL}) for the GD-0 group showed that indirect GAG interactions resulting from the stress balance hypothesis modulate peak and equilibrium stresses but not relaxation behavior (i.e., time constant and relaxation ratio) (Fig. 8). The parameter studies using averaged elastic parameters (α_1, α_2, and γ_1) for the GD-55 and GD-85 groups with COL viscous parameters (τ_1^{COL}, g_1^{COL}, τ_2^{COL}, and g_2^{COL}) for the GD-0 group showed that the additional effect of direct GAG interactions on COL elasticity further modulates peak and equilibrium stresses but not re-

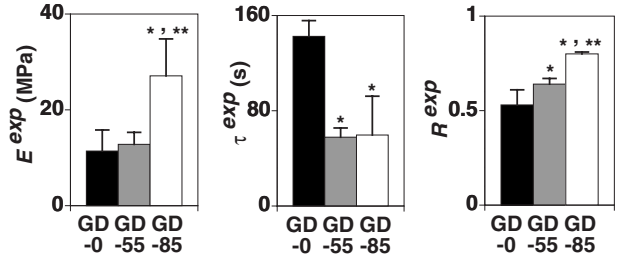

Fig. 3 The effects of GAG depletion treatment on experimental tissue VE parameters (E^{exp}, τ^{exp}, and R^{exp}): mean+1 standard deviation values shown; GD-0 is the control group with no GAG depletion; GD-55 and GD-85 are experimental groups with ~55% and 85% GAG depletion, respectively; * is the significant difference between experimental and control group values and ** is the significant difference between experimental group values (ANOVA with posthoc Tukey testing $p<0.05$)

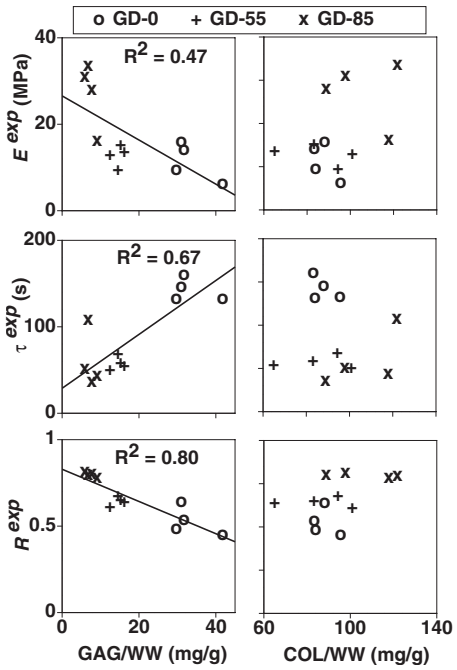

Fig. 4 Experimental tissue VE parameters (E^{exp}, τ^{exp}, and R^{exp}) versus GAG and COL contents: GD-0 is the control group with no GAG depletion; GD-55 and GD-85 are experimental groups with ~55% and 85% GAG depletion, respectively. The linear regression results were only shown for significant correlations (*t*-test analysis of regression slope, $p<0.05$).

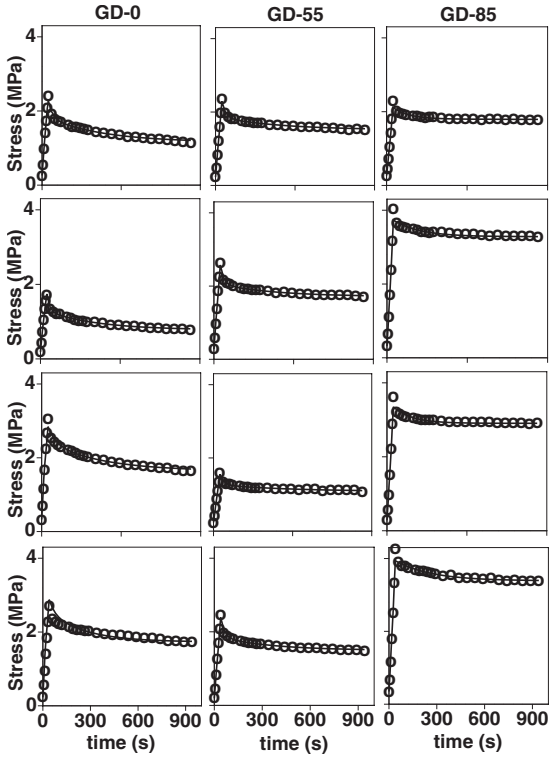

Fig. 5 Specimen-specific curve-fits of the constituent based VE model: GD-0 is the group with no GAG depletion; GD-55 and GD-85 are experimental groups with ~55% and 85% GAG depletion, respectively.

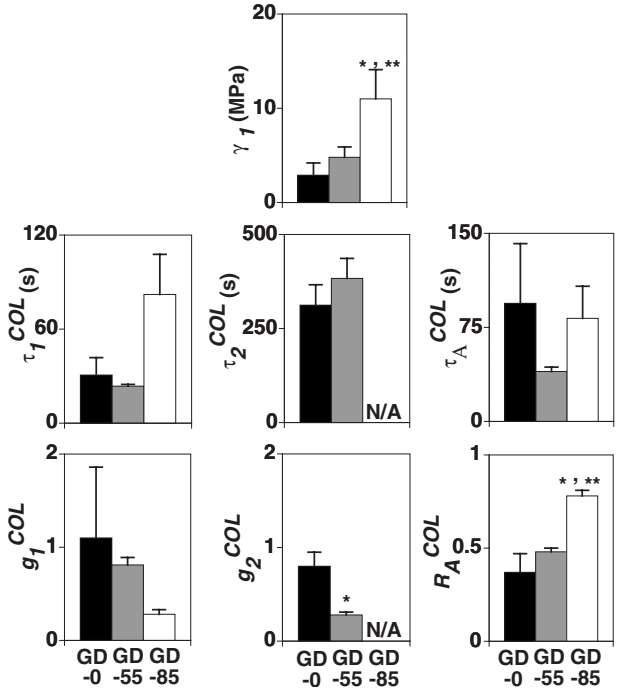

Fig. 6 The effects of GAG depletion treatment on COL VE parameters (γ_1, τ_1^{COL}, g_1^{COL}, τ_2^{COL}, g_2^{COL}, τ_A^{COL}, and R_A^{COL}); mean+1 standard deviation values were shown; GD-0 is the control group with no GAG depletion; GD-55 and GD-85 are experimental groups with ~55% and 85% GAG depletion, respectively; τ_2^{COL} and g_2^{COL} values were not reported for GD-85 specimens because only one Prony series term was used in the COL relaxation function for that group. For γ_1, τ_A^{COL}, and R_A^{COL}: * is the significant difference between experimental and control group values and ** is the significant difference between experimental group values (ANOVA with posthoc Tukey testing $p<0.05$). For τ_1^{COL}, g_1^{COL}, τ_2^{COL}, and g_2^{COL}: * is the significant difference between GD-0 and GD-55 group values (paired *t*-test $p<0.05$).

laxation behavior (Fig. 8). The simulations with all GAG and COL VE parameters for the GD-55 and GD-85 groups showed that COL VE parameters modulate relaxation behavior in addition to peak and equilibrium stresses.

4 Discussion

A constituent based nonlinear VE model for AC tissue was developed using quasilinear VE GAG and COL constituents. For uniaxial loading it was shown that this model produces a nonlinear VE response for which both the time constant and relaxation ratio are strain dependent, as opposed to a quasilinear VE response for which only the relaxation ratio is strain dependent. More specifically, the quasilinear VE relaxation ratio is strain dependent when the initial strain is not zero but is strain independent when the initial strain is zero. That conclusion highlights one mechanism that contributes to nonlinear VE properties, i.e., the presence of multiple constituents that contribute distinct VE parameters. For the UT model that neglected GAG VE for the analysis of UT experiments, it was shown that the time constant is strain independent while the relaxation ratio is strain dependent even when the initial strain is zero, in contrast to quasilinear viscoelasticity. Consequently, the UT model falls somewhere between quasilinear and nonlinear viscoelasticity.

The results for the experimental tissue VE parameters (E^{exp}, τ^{exp}, and R^{exp}) when compared with results from previous studies that included more mature AC tissue tested in UT suggest that there exist GAG-COL interactions that remodel during developmental growth. Specifically, E^{exp}/τ^{exp} values were increased/

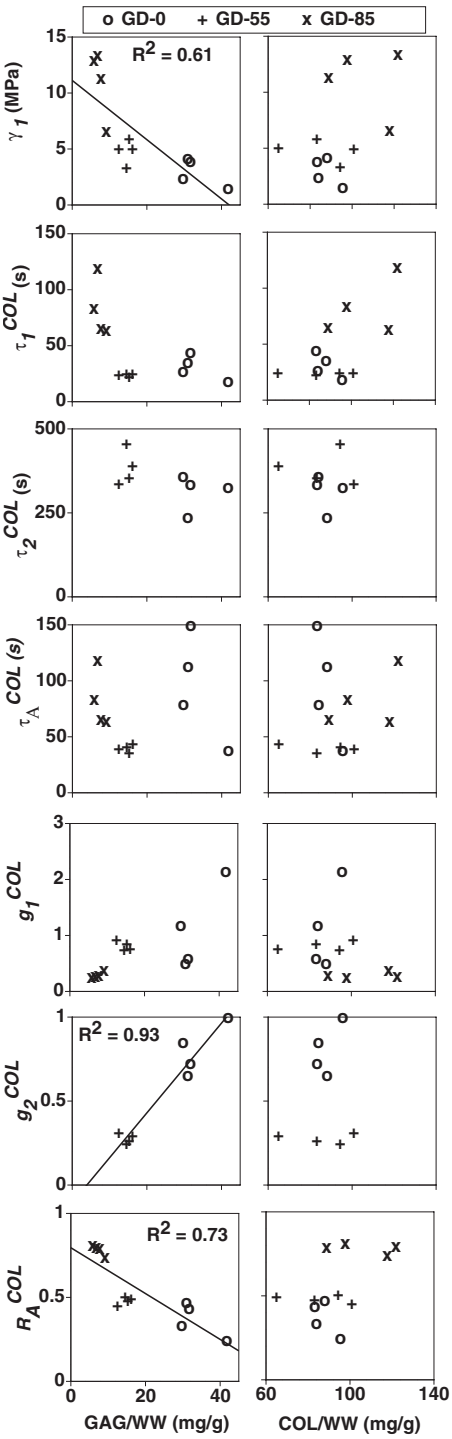

Fig. 7 COL VE parameters (γ_1, τ_1^{COL}, g_1^{COL}, τ_2^{COL}, g_2^{COL}, τ_A^{COL}, and R_A^{COL}) versus GAG and COL contents: GD-0 is the control group with no GAG depletion; GD-55 and GD-85 are experimental groups with ~55% and 85% GAG depletion, respectively. The linear regression results were only shown for significant correlations (*t*-test analysis of regression slope $p<0.05$).

decreased following GAG depletion and correlated with GAG content in this study. In contrast, E^{exp}/τ^{exp} values were maintained/decreased following GAG depletion in Ref. [26] with more mature AC tissue (18 months old bovine) and E^{exp} values were decreased following GAG depletion and not correlated with GAG content in Ref. [24,25] with adult human tissue. These differences may be due to the use of a more mature AC tissue in

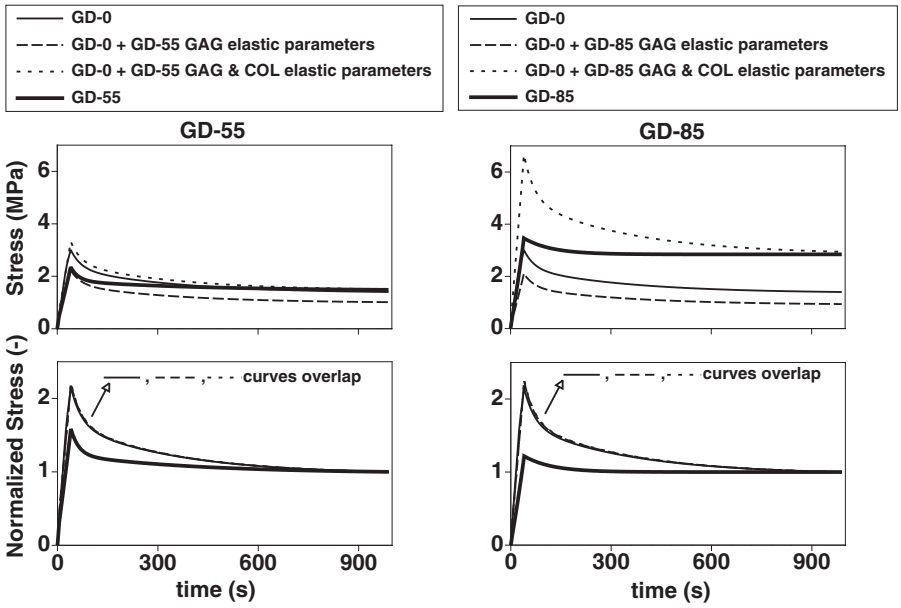

Fig. 8 The parameter study results were shown to differentiate between the different mechanisms arising from GAG-COL interactions on the experimental tissue VE response: absolute (top) and normalized (bottom) stress results for UT simulations with progressive changes in untreated (GD-0) group parameters due to treatment (GD-55, GD-85); parameters used are listed in Table 1. The stress-time curves from the first three simulations for each treatment were indistinguishable in the normalized stress plots. GAG and COL elastic parameters modulate the peak and equilibrium stresses (top) but not the relaxation behavior (bottom). COL viscous parameters modulate peak and equilibrium stresses (top) and relaxation behavior (bottom).

Refs. [24–26] than the newborn (~1–3 weeks old) bovine AC tissue used here. This hypothesis is supported by recent results that the effects of GAG depletion on tensile properties (i.e., equilibrium modulus, ramp modulus, strength, and failure strain) depend on AC tissue maturational stage [29].

In addition to the studies mentioned above for AC tissue tested in UT, GAG depleted tissue was tested in unconfined compression from mature (1–2 years old) bovine AC and modeled using small strain poroviscoelastiy [27]. Those results showed that VE time constants decreased due to GAG depletion, in agreement with the results of this study, and the unconfined compression elastic modulus decreased due to GAG depletion, in contrast with the results of this study. Again, this difference is likely due to the distinct maturational stages of the specimens.

Collectively, these results suggest that during maturation there exist GAG-COL interactions that provide for a highly compliant (i.e., low tensile modulus) SM. The biological significance of a highly compliant SM is a key property that underlies a mechanism for rapid volumetric expansion during developmental growth. Further, GAG-COL interactions may provide a lower relaxation ratio (i.e., higher peak stress for a given equilibrium stress) and enhanced viscous properties as illustrated in Fig. 8. As a creep analysis would reveal lower SM strains during repeated load applications, the biological significance of enhanced viscous properties may be that it is a mechanism that may protect cells against excessive matrix strains, that are know to cause cell death [49], during repeated loading.

A novel outcome of this study was that the experimental tissue VE response with and without GAG depletion treatment was interpreted in terms of a constituent based VE model. Although in general both GAG and COL intrinsic VE parameters may be active during complex in vivo loading conditions, in this study intrinsic GAG viscoelasticity was neglected due to the assumption that the UT VE response is dominated by intrinsic COL viscoelasticity. This assumption was invoked in previous studies [34–37] and is supported by experimental time constants and dynamic moduli measured in shear for GAG solutions [26,50,51], which were several orders of magnitude less than time constants and dynamic moduli measured for intact AC [26,52]. Those previous results, combined with the hypothesis that shear resistance is provided by tensile stresses produced in the GAG inflated COL network [53], suggest that intrinsic GAG viscoelasticity can be neglected in UT. Indeed, this assumption was supported by pilot analyses for the current study with four VE coefficients (g_1^{GAG}, τ_1^{GAG}, g_1^{COL}, and τ_1^{COL}) as unique solutions for these coefficients were not found and the best-fit solutions yielded tensile GAG stresses of ~0.3 MPa, which may not be physically relevant as GAGs are thought to provide primarily compressive resistance.[13]

If the assumption of neglecting intrinsic GAG viscoelasticity is valid, then the results of this study suggest that GAGs interact with the COL network to affect intrinsic COL viscoelasticity as select COL VE parameters changed due to GAG depletion and were correlated with GAG content. Interestingly, the GD-0 and GD-55 specimens exhibited distinct short- and long-term relaxation regimes as evidenced by the ability of the model to find unique solutions using two Prony series terms in the COL relaxation function, whereas this distinction was not possible to detect for GD-85 specimens. The parameter studies suggest that indirect GAG interactions arising from a GAG-COL stress balance as well as direct GAG interactions on COL elastic parameters modulate the peak and equilibrium stresses while direct GAG interactions on COL viscous parameters modulate the relaxation response.

Although the elastic moduli were correlated with GAG content they were not correlated with COL content, in contrast to results in Ref. [24]. The protocols, which included two treatment groups that depleted GAGs by ~55% and 85%, produced a wide range of GAG content, which made it possible to detect correlations with

[13]Also, our own pilot simulations using a poroviscoelastic model (results of which are not presented) justified the assumption that fluid flow-dependent viscoelasticity can be neglected for out UT protocols.

GAG content with a limited number of specimens in each group. However, all groups had comparable COL content making it difficult to detect correlations with COL content; since positive trends existed for $E^{\exp}$ ($p=0.19$), $R^{\exp}$ ($p=0.13$), γ_1 ($p=0.15$), and R_A^{COL} ($p=0.10$) it is likely that increasing the number of specimens would allow for the detection of correlations with COL content.

A previous study [54] suggested that although tissue VE is affected by GAG depletion for aortic valve tissue, the mechanism for such changes is decreasing water content that accompanies GAG depletion. However, additional statistical analyses for the present study (results of which are not presented) revealed no significant correlations between any of the VE parameters and water content, suggesting that GAG-COL interactions were more prominent than water-COL interactions for the experiments performed in this study.

In summary, a constituent based nonlinear VE model was developed that modified a previous model [23] and used to quantify AC tissue remodeling due to altered GAG-COL interactions. The results suggest that the GAGs interact with the COL network to affect tissue VE properties in immature AC tissue. Upon considering results from other studies with more mature tissue, it appears that GAG-COL interactions exist that may be beneficial for rapid volumetric expansion during developmental growth while protecting cells from excessive matrix strains. Furthermore, such interactions appear to diminish as the tissue matures, indicative of a remodeling response during developmental growth.

Acknowledgment

G.C.T. and S.M.K. thank Professor Pasquale Vena, Professor Alberto Redaelli, and their colleagues in the Laboratory of Biological Structure Mechanics and the Cellular and Molecular Biomechanics Research Group, respectively, for hosting their research visit at Politecnico di Milano from July 2007 to February 2008. The funding of the research was received from the National Science Foundation (R.L.S. and S.M.K.), the National Institutes of Health (R.L.S. and S.M.K.), and the Howard Hughes Medical Institute (UCSD for R.L.S.).

Appendix A

The elastic stress constitutive law is based on a bimodular polyconvex fiber-reinforced anisotropic strain energy function for AC [40] where an isotropic GAG matrix is reinforced with a COL fiber constituent. The elastic GAG stress ${}^e\mathbf{S}^{\mathrm{GAG}}$ is based on a two compartmental (i.e., extra- and intrafibrillar water compartments) isotropic swelling stress model for AC GAGs originally proposed in Ref. [38] and used in Refs. [5,39] to derive the polyconvex continuum level model

$$ {}^e\mathbf{S}^{\mathrm{GAG}} = -\frac{\alpha_1}{(J^{\mathrm{GAG}})^{\alpha_2-1}}\mathbf{C}^{\mathrm{GAG}} \tag{A1} $$

where α_1 and α_2 are material constants.

The elastic COL stress ${}^e\mathbf{S}^{\mathrm{COL}}$ is based on Ref. [40] and contains both an isotropic component ${}^e\mathbf{S}^0$ and a anisotropic bimodular component ${}^e\mathbf{S}^{\mathrm{BIM}}$:

$$ {}^e\mathbf{S}^{\mathrm{COL}} = {}^e\mathbf{S}^0 + {}^e\mathbf{S}^{\mathrm{BIM}} \tag{A2} $$

${}^e\mathbf{S}^0$ is defined as

$$ {}^e\mathbf{S}^0 = \mu(\mathbf{I} - (\mathbf{C}^{\mathrm{COL}})^{-1}) \tag{A3} $$

where μ is a material constant and -1 denotes an inverse operator. The fiber reinforcement of the SM appears in ${}^e\mathbf{S}^{\mathrm{BIM}}$. In this model, there are three primary fiber directions along mutually orthogonal unit vectors $\mathbf{E}_1$, $\mathbf{E}_2$, and $\mathbf{E}_3$, which generate structural tensors

$$ \mathbf{M}_1 = \mathbf{E}_1 \otimes \mathbf{E}_1, \quad \mathbf{M}_2 = \mathbf{E}_2 \otimes \mathbf{E}_2, \quad \mathbf{M}_3 = \mathbf{E}_3 \otimes \mathbf{E}_3 \tag{A4} $$

where $\otimes$ is the dyadic product. Also, there are two secondary fiber directions in each of the three planes created by the primary unit vectors $\mathbf{E}_1$, $\mathbf{E}_2$, and $\mathbf{E}_3$ (planes 1-2, 2-3, and 1-3) along unit vectors ($\mathbf{E}_{\pm 12}$, $\mathbf{E}_{\pm 23}$, and $\mathbf{E}_{\pm 13}$) defined by angles ($\Phi_{\pm 12}$, $\Phi_{\pm 23}$, and $\Phi_{\pm 13}$) as

$$ \begin{aligned} \mathbf{E}_{\pm 12} &= \cos\Phi_{\pm 12}\mathbf{E}_1 \pm \sin\Phi_{\pm 12}\mathbf{E}_2 \\ \mathbf{E}_{\pm 23} &= \cos\Phi_{\pm 23}\mathbf{E}_2 \pm \sin\Phi_{\pm 23}\mathbf{E}_3 \\ \mathbf{E}_{\pm 13} &= \cos\Phi_{\pm 13}\mathbf{E}_1 \pm \sin\Phi_{\pm 13}\mathbf{E}_3 \end{aligned} \tag{A5} $$

These generate structural tensors

$$ \begin{aligned} \mathbf{M}_{\pm 12} &= \cos^2\phi_{12}\mathbf{E}_1 \otimes \mathbf{E}_1 + \sin^2\phi_{12}\mathbf{E}_2 \otimes \mathbf{E}_2 \\ &\quad \pm \cos\phi_{12}\sin\phi_{12}(\mathbf{E}_1 \otimes \mathbf{E}_2 + \mathbf{E}_2 \otimes \mathbf{E}_1) \\ \mathbf{M}_{\pm 23} &= \cos^2\phi_{23}\mathbf{E}_2 \otimes \mathbf{E}_2 + \sin^2\phi_{23}\mathbf{E}_3 \otimes \mathbf{E}_3 \\ &\quad \pm \cos\phi_{12}\sin\phi_{12}(\mathbf{E}_2 \otimes \mathbf{E}_3 + \mathbf{E}_3 \otimes \mathbf{E}_2) \\ \mathbf{M}_{\pm 13} &= \cos^2\phi_{13}\mathbf{E}_1 \otimes \mathbf{E}_1 + \sin^2\phi_{13}\mathbf{E}_3 \otimes \mathbf{E}_3 \\ &\quad \pm \cos\phi_{13}\sin\phi_{13}(\mathbf{E}_1 \otimes \mathbf{E}_3 + \mathbf{E}_3 \otimes \mathbf{E}_1) \end{aligned} \tag{A6} $$

The strain energy function W^{BIM} is modified from Ref. [40] to model a linear stress-strain response typical of newborn bovine tissue. The resulting expression for ${}^e\mathbf{S}^{\mathrm{BIM}}$ is

$$ \begin{aligned} {}^e\mathbf{S}^{\mathrm{BIM}} &= \left(\sum_{i=1}^{3}\gamma_i[\lambda_i^2](\lambda_i^2-1)\mathbf{M}_i\right) + \delta[\lambda_{\pm 12}^2](\lambda_{\pm 12}^2-1)\mathbf{M}_{\pm 12} \\ &\quad + \delta[\lambda_{\pm 23}^2](\lambda_{\pm 23}^2-1)\mathbf{M}_{\pm 23} + \delta[\lambda_{\pm 13}^2](\lambda_{\pm 13}^2-1)\mathbf{M}_{\pm 13} \end{aligned} \tag{A7} $$

where λ_i^2 terms represent the component of $\mathbf{C}^{\mathrm{COL}}$ in the ith direction (i.e., $\mathbf{M}_1 \cdot \mathbf{C}^{\mathrm{COL}}$, etc.) and $\lambda_{\pm 12}^2$, $\lambda_{\pm 23}^2$, and $\lambda_{\pm 13}^2$ represent the squared stretch in the secondary fiber directions (i.e., $\mathbf{M}_{+12} \cdot \mathbf{C}^{\mathrm{COL}}$, etc.). The material constants γ_1, γ_2, γ_3, and δ implement the bimodular feature with the following definitions:[14]

$$ \begin{aligned} \gamma_i[\lambda_i^2] &= \begin{cases} \gamma_i & \text{for } \lambda_i^2 \geq 1 \\ 0 & \text{for } \lambda_i^2 < 1 \end{cases} \\ \delta[\lambda_{+12}^2] &= \begin{cases} \delta & \text{for } \lambda_{+12}^2 \geq 1 \\ 0 & \text{for } \lambda_{+12}^2 < 1 \end{cases}, \quad \text{etc.} \end{aligned} \tag{A8} $$

Appendix B

Recall Eq. (8) for the loading stress S for UT with a single constituent

$$ S(t) = {}^eS(0) + \int_0^t G(t-\tau)\frac{d^eS}{d\tau}d\tau \tag{B1} $$

For a step increase in elastic stress Δ^eS at time $t_{\mathrm{step}} > 0$ with initial equilibrium elastic stress ${}^eS(0)$, the elastic stress response is represented with the Heaviside step function $H(t, t_{\mathrm{step}})$

$$ \begin{aligned} {}^eS(t) &= {}^eS(0) + H(t, t_{\mathrm{step}})\Delta^eS \quad \text{where} \\ H(t, t_{\mathrm{step}}) &= \begin{cases} 0 & \text{for } t < t_{\mathrm{step}} \\ 1 & \text{for } t \geq t_{\mathrm{step}} \end{cases} \end{aligned} \tag{B2} $$

so that

[14] It can be seen from Eq. (A8) that when a COL fiber direction is not stretched in tension, it is "turned off" and does not contribute to ${}^e\mathbf{S}^{\mathrm{BIM}}$.

$$\frac{d^e S}{d\tau} = \Delta^e S \delta(\tau, t_{\text{step}}) \quad \text{where} \quad \delta(t, t_{\text{step}}) = \begin{cases} \infty & \text{for } t = t_{\text{step}} \\ 0 & \text{for } t \neq t_{\text{step}} \end{cases} \tag{B3}$$

where $\delta(t, t_{\text{step}})$ is the unit impulse function. When $t > t_{\text{step}}$, the convolution integral in Eq. (B1) can be evaluated by separating the integration limits at t_{step}^-, defined as the moment before the instantaneous step

$$\int_0^t G(t-\tau)\frac{d^e S}{d\tau}d\tau = \int_0^{t_{\text{step}}^-} G(t-\tau)\Delta^e S \delta(\tau, t_{\text{step}})d\tau + \int_{t_{\text{step}}^-}^t G(t-\tau)\Delta^e S \delta(\tau, t_{\text{step}})d\tau \tag{B4}$$

where the first term on the right side of Eq. (B4) is zero because the unit impulse function is zero for $t \neq t_{\text{step}}$. Using an expression for $G(t\text{-}\tau)$ from Eq. (7) in Eq. (B4) yields

$$\int_0^t G(t-\tau)\frac{d^e S}{d\tau}d\tau = \int_{t_{\text{step}}^-}^t \Delta^e S \delta(\tau, t_{\text{step}})d\tau + \int_{t_{\text{step}}^-}^t \sum_{i=1}^n g_i \exp\left(\frac{-(t-\tau)}{\tau_i}\right)\Delta^e S \delta(\tau, t_{\text{step}})d\tau \tag{B5}$$

By noting the integral of the unit impulse function is the Heaviside step function, the first term on the right side of Eq. (B5) becomes

$$\int_{t_{\text{step}}^-}^t \Delta^e S \delta(\tau, t_{\text{step}})d\tau = \Delta^e S H(\tau, t_{\text{step}})\Big|_{\tau=t_{\text{step}}^-}^{\tau=t} = \Delta^e S \tag{B6}$$

The following equation is needed to integrate the product of a function $f(t)$ and the impulse function $\delta(t,a)$.

$$\int_{-d}^{d} \delta(t,a) f(t) dt = f(a) \quad \text{for} \quad -\infty \leq -d < a < d \leq \infty \tag{B7}$$

Using Eq. (B7) the second term on the right side of Eq. (B5) becomes

$$\int_{t_{\text{step}}^-}^t \sum_{i=1}^n g_i \exp\left(\frac{-(t-\tau)}{\tau_i}\right)\Delta^e S \delta(\tau, t_{\text{step}})d\tau = \Delta^e S \sum_{i=1}^n g_i \exp\left(\frac{-(t-t_{\text{step}})}{\tau_i}\right) \tag{B8}$$

By substituting Eqs. (B5), (B6), and (B8) into Eq. (B1) yields the stress at $t \geq t_{\text{step}}$

$$\mathbf{S}(t) = {}^e\mathbf{S}(0) + \Delta^e\mathbf{S} + \Delta^e\mathbf{S}\sum_{i=1}^n g_i \exp\left(\frac{-(t-t_{\text{step}})}{\tau_i}\right) \tag{B9}$$

References

[1] Linn, F. C., and Sokoloff, L., 1965, "Movement and Composition of Interstitial Fluid of Cartilage," Arthritis Rheum., **8**, pp. 481–494.

[2] Buckwalter, J., Hunziker, E., Rosenberg, L., Coutts, R., Adams, M., and Eyre, D., 1988, "Articular Cartilage: Composition and Structure," *Injury and Repair of the Musculoskeletal Soft Tissues*, S. L.-Y. Woo and J. A. Buckwalter, eds., American Academy of Orthopaedic Surgeons, Park Ridge, IL, pp. 405–425.

[3] Mow, V. C., and Ratcliffe, A., 1997, "Structure and Function of Articular Cartilage and Meniscus," *Basic Orthopaedic Biomechanics*, V. C. Mow and W. C. Hayes, eds., Raven, New York, pp. 113–178.

[4] Klisch, S. M., Chen, S. S., Sah, R. L., and Hoger, A., 2003, "A Growth Mixture Theory for Cartilage With Applications to Growth-Related Experiments on Cartilage Explants," ASME J. Biomech. Eng., **125**, pp. 169–179.

[5] Klisch, S. M., Asanbaeva, A., Oungoulian, S. R., Thonar, E. J., Masuda, K., Davol, A., and Sah, R. L., 2008, "A Cartilage Growth Mixture Model With Collagen Remodeling: Validation Protocols," ASME J. Biomech. Eng., **130**, p. 031006.

[6] Schinagl, R. M., Gurskis, D., Chen, A. C., and Sah, R. L., 1997, "Depth-Dependent Confined Compression Modulus of Full-Thickness Bovine Articular Cartilage," J. Orthop. Res., **15**, pp. 499–506.

[7] Huang, C. Y., Stankiewicz, A., Ateshian, G. A., and Mow, V. C., 2005, "Anisotropy, Inhomogeneity, and Tension-Compression Nonlinearity of Human Glenohumeral Cartilage in Finite Deformation," J. Biomech., **38**(4), pp. 799–809.

[8] Soltz, M. A., and Ateshian, G. A., 2000, "A Conewise Linear Elasticity Mixture Model for the Analysis of Tension-Compression Nonlinearity in Articular Cartilage," ASME J. Biomech. Eng., **122**, pp. 576–586.

[9] Laasanen, M., Toyras, J., Korhonen, R., Rieppo, J., Saarakkala, S., Nieminen, M., Hirvonen, J., and Jurvelin, J. S., 2003, "Biomechanical Properties of Knee Articular Cartilage," Biorheology, **40**, pp. 133–140.

[10] Donzelli, P. S., Spilker, R. L., Ateshian, G. A., and Mow, V. C., 1999, "Contact Analysis of Biphasic Transversely Isotropic Cartilage Layers and Correlations With Tissue Failure," J. Biomech., **32**(10), pp. 1037–1047.

[11] Krishnan, R., Park, S., Eckstein, F., and Ateshian, G. A., 2003, "Inhomogeneous Cartilage Properties Enhance Superficial Insterstitial Fluid Support and Frictional Properties, but Do Not Provide a Homogeneous State of Stress," ASME J. Biomech. Eng., **125**(5), pp. 569–577.

[12] Mak, A. F., 1986, "The Apparent Viscoelastic Behavior of Articular Cartilage—The Contributions From the Intrinsic Matrix Viscoelasticity and Interstitial Fluid Flows," ASME J. Biomech. Eng., **108**, pp. 123–130.

[13] Suh, J.-K., and DiSilvestro, M. R., 1999, "Biphasic Poroviscoelastic Behavior of Hydrated Biological Soft Tissue," ASME J. Appl. Mech., **66**, pp. 528–535.

[14] Huang, C. Y., Mow, V. C., and Ateshian, G. A., 2001, "The Role of Flow-Independent Viscoelasticity in the Biphasic Tensile and Compressive Responses of Articular Cartilage," ASME J. Biomech. Eng., **123**(5), pp. 410–417.

[15] Korhonen, R. K., Laasanen, M. S., Toyras, J., Lappalainen, R., Helminen, H. J., and Jurvelin, J. S., 2003, "Fibril Reinforced Poroelastic Model Predicts Specifically Mechanical Behavior of Normal, Proteoglycan Depleted and Collagen Degraded Articular Cartilage," J. Biomech., **36**(9), pp. 1373–1379.

[16] Wilson, W., van Donkelaar, C. C., van Rietbergen, B., Ito, K., and Huiskes, R., 2004, "Stresses in the Local Collagen Network of Articular Cartilage: A Poroviscoelastic Fibril-Reinforced Finite Element Study," J. Biomech., **37**, pp. 357–366.

[17] Garcia, J. J., and Cortes, D. H., 2006, "A Nonlinear Biphasic Viscohyperelastic Model for Articular Cartilage," J. Biomech., **39**(16), pp. 2991–2998.

[18] Fung, Y. C., 1972, "Stress-Strain History Relations of Soft Tissues in Simple Elongation," *Biomechanics: Its Foundations and Objectives*, Y. C. Fung, N. Perrone, and M. Anliker, eds., Prentice-Hall, Englewood Cliffs, NJ, pp. 181–208.

[19] Provenzano, P., Lakes, R., Keenan, T., and Vanderby, R., Jr., 2001, "Nonlinear Ligament Viscoelasticity," Ann. Biomed. Eng., **29**(10), pp. 908–914.

[20] Suh, J. K., and Bai, S., 1998, "Finite Element Formulation of Biphasic Poroviscoelastic Model for Articular Cartilage," ASME J. Biomech. Eng., **120**, pp. 195–201.

[21] DiSilvestro, M. R., and Suh, J. K., 2001, "A Cross-Validation of the Biphasic Poroviscoelastic Model of Articular Cartilage in Unconfined Compression, Indentation, and Confined Compression," J. Biomech., **34**(4), pp. 519–525.

[22] Park, S., and Ateshian, G. A., 2006, "Dynamic Response of Immature Bovine Articular Cartilage in Tension and Compression, and Nonlinear Viscoelastic Modeling of the Tensile Response," ASME J. Biomech. Eng., **128**(4), pp. 623–630.

[23] Vena, P., Gastaldi, D., and Contro, R., 2006, "A Constituent-Based Model for the Nonlinear Viscoelastic Behavior of Ligaments," ASME J. Biomech. Eng., **128**, pp. 449–457.

[24] Kempson, G. E., Muir, H., Pollard, C., and Tuke, M., 1973, "The Tensile Properties of the Cartilage of Human Femoral Condyles Related to the Content of Collagen and Glycosaminoglycans," Biochim. Biophys. Acta, **297**, pp. 456–472.

[25] Kempson, G. E., Tuke, M. A., Dingle, J. T., Barrett, A. J., and Horsfield, P. H., 1976, "The Effects of Proteolytic Enzymes on the Mechanical Properties of Adult Human Articular Cartilage," Biochim. Biophys. Acta, **428**, pp. 741–760.

[26] Schmidt, M. B., Mow, V. C., Chun, L. E., and Eyre, D. R., 1990, "Effects of Proteoglycan Extraction on the Tensile Behavior of Articular Cartilage," J. Orthop. Res., **8**, pp. 353–363.

[27] DiSilvestro, M. R., and Suh, J. K., 2002, "Biphasic Poroviscoelastic Characteristics of Proteoglycan-Depleted Articular Cartilage: Simulation of Degeneration," Ann. Biomed. Eng., **30**(6), pp. 792–800.

[28] Asanbaeva, A., Masuda, K., Thonar, E. J.-M. A., Klisch, S. M., and Sah, R. L., 2007, "Mechanisms of Cartilage Growth: Modulation of Balance Between Proteoglycan and Collagen In Vitro Using Chondroitinase ABC," Arthritis Rheum., **56**, pp. 188–198.

[29] Asanbaeva, A., Tam, J., Schumacher, B. L., Klisch, S. M., Masuda, K., and Sah, R. L., 2008, "Articular Cartilage Tensile Integrity: Modulation by Matrix Depletion Is Maturation-Dependent," Arch. Biochem. Biophys., **474**(1), pp. 175–182.

[30] Al Jamal, R., Roughley, P. J., and Ludwig, M. S., 2001, "Effect of Glycosaminoglycan Degradation on Lung Tissue Viscoelasticity," Am. J. Physiol. Lung Cell. Mol. Physiol., **280**(2), pp. L306–315.

[31] Tanaka, E., Aoyama, J., Tanaka, M., Van Eijden, T., Sugiyama, M., Hanaoka, K., Watanabe, M., and Tanne, K., 2003, "The Proteoglycan Contents of the Temporomandibular Joint Disc Influence Its Dynamic Viscoelastic Properties," J. Biomed. Mater. Res. Part A, **65**(3), pp. 386–392.
[32] Elliott, D. M., Robinson, P. S., Gimbel, J. A., Sarver, J. J., Abboud, J. A., Iozzo, R. V., and Soslowsky, L. J., 2003, "Effect of Altered Matrix Proteins on Quasilinear Viscoelastic Properties in Transgenic Mouse Tail Tendons," Ann. Biomed. Eng., **31**(5), pp. 599–605.
[33] Liao, J., and Vesely, I., 2004, "Relationship Between Collagen Fibrils, Glycosaminoglycans, and Stress Relaxation in Mitral Valve Chordae Tendineae," Ann. Biomed. Eng., **32**(7), pp. 977–983.
[34] Li, L. P., and Herzog, W., 2004, "The Role of Viscoelasticity of Collagen Fibers in Articular Cartilage: Theory and Numerical Formulation," Biorheology, **41**(3–4), pp. 181–194.
[35] Li, L. P., Herzog, W., Korhonen, R. K., and Jurvelin, J. S., 2005, "The Role of Viscoelasticity of Collagen Fibers in Articular Cartilage: Axial Tension Versus Compression," Med. Eng. Phys., **27**(1), pp. 51–57.
[36] Wilson, W., van Donkelaar, C. C., van Rietbergen, B., and Huiskes, R., 2005, "A Fibril-Reinforced Poroviscoelastic Swelling Model for Articular Cartilage," J. Biomech., **38**(6), pp. 1195–1204.
[37] Garcia, J. J., and Cortes, D. H., 2007, "A Biphasic Viscohyperelastic Fibril-Reinforced Model for Articular Cartilage: Formulation and Comparison With Experimental Data," J. Biomech., **40**(8), pp. 1737–1744.
[38] Basser, P. J., Schneiderman, R., Bank, R. A., Wachtel, E., and Maroudas, A., 1998, "Mechanical Properties of the Collagen Network in Human Articular Cartilage as Measured by Osmotic Stress Technique," Arch. Biochem. Biophys., **351**, pp. 207–219.
[39] Oungoulian, S. R., Chen, S. S., Davol, A., Sah, R. L., and Klisch, S. M., 2007, "Extended Two-Compartmental Swelling Stress Model and Isotropic Cauchy Stress Equation for Articular Cartilage Proteoglycans," ASME Summer Bioengineering Conference, Keystone, CO.
[40] Klisch, S. M., 2007, "A Bimodular Polyconvex Anisotropic Strain Energy Function for Articular Cartilage," ASME J. Biomech. Eng., **129**, pp. 250–258.
[41] Asanbaeva, A., 2006, "Cartilage Growth and Remodeling: Modulation of Growth Phenotype and Tensile Integrity," Ph.D. thesis, University of California, La Jolla, San Diego, CA.
[42] Williamson, A. K., Chen, A. C., Masuda, K., Thonar, E. J.-M. A., and Sah, R. L., 2003, "Tensile Mechanical Properties of Bovine Articular Cartilage: Variations With Growth and Relationships to Collagen Network Components," J. Orthop. Res., **21**, pp. 872–880.
[43] Williamson, A. K., Masuda, K., Thonar, E. J.-M. A., and Sah, R. L., 2003, "Growth of Immature Articular Cartilage In Vitro: Correlated Variation in Tensile Biomechanical and Collagen Network Properties," Tissue Eng., **9**, pp. 625–634.
[44] Farndale, R. W., Buttle, D. J., and Barrett, A. J., 1986, "Improved Quantitation and Discrimination of Sulphated Glycosaminoglycans by Use of Dimethylmethylene Blue," Biochim. Biophys. Acta, **883**, pp. 173–177.
[45] Woessner, Jr., J. F., 1961, "The Determination of Hydroxyproline in Tissue and Protein Samples Containing Small Proportions of This Imino Acid," Arch. Biochem. Biophys., **93**, pp. 440–447.
[46] Kim, Y. J., Sah, R. L. Y., Doong, J. Y. H., and Grodzinsky, A. J., 1988, "Fluorometric Assay of DNA in Cartilage Explants Using Hoechst 33258," Anal. Biochem., **174**, pp. 168–176.
[47] Sasazaki, Y., Shore, R., and Seedhom, B. B., 2004, "Ultrastructure of Cartilage Under Tensile Strain," Transactions of the 50th Annual Meeting, Orthopaedic Research Society, **29**, pp. 606.
[48] Ficklin, T. P., Thomas, G. C., Barthel, J. C., Asanbaeva, A., Thonar, E. J., Masuda, K., Chen, A. C., Sah, R. L., Davol, A., and Klisch, S. M., 2007, "Articular Cartilage Mechanical and Biochemical Property Relations Before and After In Vitro Growth," J. Biomech., **40**, pp. 3607–3614.
[49] Morel, V., and Quinn, T. M., 2004, "Cartilage Injury by Ramp Compression Near the Gel Diffusion Rate," J. Orthop. Res., **22**, pp. 145–151.
[50] Hardingham, T. E., Muir, H., Kwan, M. K., Lai, W. M., and Mow, V. C., 1987, "Viscoelastic Properties of Proteoglycan Solutions With Varying Proportions Present as Aggregates," J. Orthop. Res., **5**, pp. 36–46.
[51] Mow, V. C., Mak, A. F., Lai, W. M., Rosenberg, L. C., and Tang, L. H., 1984, "Viscoelastic Properties of Proteoglycan Subunits and Aggregates in Varying Solution Concentrations," J. Biomech., **17**(5), pp. 325–338.
[52] Spirt, A. A., Mak, A. F., and Wassell, R. P., 1989, "Nonlinear Viscoelastic Properties of Articular Cartilage in Shear," J. Orthop. Res., **7**, pp. 43–49.
[53] Zhu, W., Mow, V. C., Koob, T. J., and Eyre, D. R., 1993, "Viscoelastic Shear Properties of Articular Cartilage and the Effects of Glycosidase Treatment," J. Orthop. Res., **11**, pp. 771–781.
[54] Bhatia, A., and Vesely, I., 2005, "The Effect of Glycosaminoglycans and Hydration on the Viscoelastic Properties of Aortic Valve Cusps," Conf. Proc. IEEE Eng. Med. Biol. Soc., **3**, pp. 2979–2980.